Experimental and modeling study on the transient flow and time-dependent yield stress of superfine-tailings cemented paste backfill

Guo, Zhenbang; Qiu, Jingping; Jiang, Haiqiang; Zhu, Qiang; Wang Kwek, Jin; Ke, Lin; Qu, Zhengyao

DOI
10.1016/j.conbuildmat.2023.130363

Publication date
2023

Document Version
Final published version

Published in
Construction and Building Materials

Citation (APA)
Guo, Z., Qiu, J., Jiang, H., Zhu, Q., Wang Kwek, J., Ke, L., & Qu, Z. (2023). Experimental and modeling study on the transient flow and time-dependent yield stress of superfine-tailings cemented paste backfill. *Construction and Building Materials*, *367*, Article 130363. https://doi.org/10.1016/j.conbuildmat.2023.130363

Construction and Building Materials 367 (2023) 130363

Contents lists available at ScienceDirect

Construction and Building Materials

journal homepage: www.elsevier.com/locate/conbuildmat

Experimental and modeling study on the transient flow and time-dependent yield stress of superfine-tailings cemented paste backfill

Zhenbang Guo [a,b,c], Jingping Qiu [a,b], Haiqiang Jiang [d], Qiang Zhu [e,f,g], Jin Wang Kwek [g], Lin Ke [e], Zhengyao Qu [e,g,*]

[a] School of Resource and Civil Engineering, Northeastern University, Shenyang, China
[b] Science and Technology Innovation Center of Smart Water and Resource Environment, Northeastern University, Shenyang 110819, China
[c] Faculty of Civil Engineering and Geosciences, Department of Hydraulic Engineering, Delft University of Technology, Stevinweg 1, 2628, CN, Delft, the Netherlands
[d] Key Laboratory of Ministry of Education on Safe Mining of Deep Metal Mines, Northeastern University, Shenyang, China
[e] Institute of Materials Research and Engineering, Agency for Science Technology and Research, Singapore 138634, Singapore
[f] School of Chemistry, Chemical Engineering and Biotechnology, Nanyang Technological University, 21 Nanyang Link, Singapore 637371 Singapore
[g] Institute of Sustainability for Chemicals, Energy and Environment, Agency for Science Technology and Research, 1 Pesek Road, Jurong Island, Singapore 627833, Singapore

ARTICLE INFO

Keywords:
Superfine-tailings cemented paste backfill
Thixotropy
Pre-shear time
Rheological model
Static yield stress

ABSTRACT

The fresh superfine-tailings cemented paste backfill (SCPB) exhibits strong thixotropy, but quantification of the resulting transient flow (non-steady state) and time-dependent yield stress is lacking. In this study, a simple qualitative model was developed to describe the transient flow and time-dependent yield stress of SCPB. The effect of pre-shear time on the rheological behavior of SCPB was investigated. In addition, the adaptability of conventional non-Newtonian rheological models to SCPB was also evaluated. The results showed the Herschel-Bulkley model provides the most stable dynamic yield stress estimation of SCPB compared to the Bingham and modified Bingham models. A longer pre-shear time (within 500 s) led to smaller initial static yield stress and delayed recovery kinetics of static yield stress, but hardly affected the steady state of SCPB and the time required to reach it. The proposed model provides a good quantification of the transient flow at a given shear rate and time-dependent yield stress of SCPB.

1. Introduction

The cemented paste backfill (CPB) technology has now become the mainstream in the global mining industry due to its eco-friendly and production-enhancing features [1]. Its main benefits include efficient disposal of tailings waste [2], filling of mine stopes [3], providing ground support [4], improving the working environment [5] and enhancing mineral recovery [6]. CPB is a composite cement-based material that typically consists of dewatered tailings, hydraulic binder and mixing water [7]. The solids content of CPB is usually 70–85 % and the binder dosage typically ranges from 2 to 9 % [8].

The mining of low-grade ores has become a general trend due to the increasing shortage of high-quality ore deposits [9]. To improve mineral recovery, more sophisticated techniques such as super-fine grinding is employed, which inevitably leads to superfine-tailings (ST, >80 % below 20 μm) by-products [10]. The flowability of CPB made from ST, also known as superfine-tailings cemented paste backfill (SCPB), is very poor due to the tendency to form flocs that trap free water [11]. This is not conducive to pipeline transportation of SCPB and may even lead to pipeline clogging, thus bringing economic losses to mine production [12]. Therefore, it is of great significance to study the flowability of SCPB for mine production. The rheological properties (including thixotropy) can be used to better illustrate the flowability, pumpability, pouring and casting processes of fresh CPB and are a prerequisite for an in-depth understanding of fresh properties of CPB [13].

Thixotropy describes the decreasing apparent viscosity with time when shearing is applied while the damaged structure can recover its initial state following a long enough resting [14]. Shear thinning and yield stress evolution can be considered as special cases of thixotropy, i.e., representing the structural breakdown and the evolution of the equilibrium structure, respectively [15]. SCPB exhibits stronger thixotropy than conventional CPB especially due to the high superfine particle

* Corresponding author at: Institute of Materials Research and Engineering, Agency for Science Technology and Research, Singapore 138634, Singapore.
E-mail address: zhengyao_qu@imre.a-star.edu.sg (Z. Qu).

https://doi.org/10.1016/j.conbuildmat.2023.130363
Received 26 October 2022; Received in revised form 5 January 2023; Accepted 8 January 2023
Available online 13 January 2023

content [16]. Therefore, thixotropy has important implications for the workability of SCPB. Some properties of SCPB, especially the transient flow (non-steady rheological response under a given shear action) and time-dependent yield stress, are mainly controlled by the thixotropy [17,18]. On the one hand, a full understanding of transient flow behavior is required for the design and operation of mixing and pumping system since fresh paste is subjected to high shear rates during production and pumping [19]. Due to the delay in the material response caused by thixotropy, there is a transient regime between two successive steady states, which cannot be adequately described by conventional non-Newtonian rheological models [20]. Thus, understanding the transient flow is also crucial to obtain accurate rheological parameters of SCPB, especially the yield stress. A large number of experiments have been carried out to study the influence of certain factors (such as particle size [21], solids content [13], curing time [22] and temperature [19], etc.) on the transient flow of CPB or SCPB. Clearly, these studies provide insight on understanding the transient flow characteristics of CPB or SCPB. However, it should be noted that the quantitative model study on transient flow characteristics of SCPB is seldomly reported. As for the time-dependent rheological properties, especially the evolution of the static yield stress, this is directly related to the structural build-up of SCPB. A pronounced structural build-up can contribute to hinder the segregation of coarse particles and thus ensure the stability of the paste [17]. Moreover, the transportation time of the paste increased continuously with increasing mining depth [23]. Therefore, a good knowledge on the time-dependent yield stress of SCPB is crucial for slurry stability and transportation. Current research into the time-dependent yield stress of CPB or SCPB has focused on the effects of certain factors (e.g., superplasticizer dosage [24], silicate modulus [25], particle size [21] and flocculants content [23]). These studies have provided considerable insight into understanding the time-dependent rheological properties of SCPB. However, the quantification and prediction of the time-dependent yield stress of SCPB need to be further explored. In summary, given the high thixotropy of SCPB and the current lack of quantitative studies on its transient flow and time-dependent yield stress or microstructure build-up, it is necessary to construct a quantitative model that meets the requirements.

As previously mentioned, SCPB is highly thixotropic, which will inevitably lead to its rheological measurements being very sensitive to the shear history. Depending on the rheological measurement protocol used, the pre-shear step prior to the measurement will last for different periods of time. The difference in pre-shear directly affects the transient flow of SCPB under the same shear and the yield stress evolution at rest. This is relevant for the measurement of rheological parameters and even for the final mix proportion design of the SCPB. Thus, it is critical to know how pre-shear durations influence the rheological behavior of fresh paste systems especially the highly thixotropic SCPB. Some studies [26,27] have focused on the effect of mixing time on the rheological properties of CPB, which provides a reference for research related to pre-shear time. However, these studies are all specific to CPB, and further exploration is needed regarding the effect of pre-shear time on the rheological properties of SCPB, especially transient flow and time dependency.

In this study, a simple thixotropy model is proposed to describe the transient flow and time-dependent yield stress of SCPB. Then, we determine the model parameters based on the results of different constant shear rate tests. Finally, we use the proposed model to evaluate the influence of pre-shear time on the transient flow and time-dependent static yield stress of SCPB.

2. Materials and experimental methods

2.1. Raw materials

The raw materials for the preparation of SCPB mainly include ST (superfine-tailings), hydraulic binder and mixing water. The ST used was obtained by grinding iron tailings from an iron ore mine in northeastern China. The particle size distribution of ST measured by laser diffraction (Mastersizer 2000, Malvern Panalytical, U.K.) can be seen in Fig. 1. The volume content of tailings with size less than 20 μm in ST (fines content) is 85.95 %, which can be considered as ST [16]. The uniformity coefficient (*Cu*) and coefficient of curvature (*Cv*) of ST are 5.39 and 1.04, respectively, which indicated that ST has a relatively good particle size distribution as stated in [28]. The X-ray fluorescence (XRF) results showed that the main chemical composition of ST is SiO_2 (75.76 %), MgO (16.10 %) and Fe_2O_3 (11.54 %), etc. In addition, the X-ray diffraction (XRD) analysis indicated that the main crystalline phases in ST are quartz, amphibole, mica and endenite. The binder agent used in this study is a commercial ordinary Portland cement (OPC), type PO 42.5R. The particle size distribution of OPC is also shown in Fig. 1, and its fines content is about 66.3 % lower than that of ST. The specific surface area, *Cu* and *Cv* of OPC are 5808 cm^2/g, 3.29 and 1.25, respectively. Additional information about OPC, such as chemical composition, can be found in [28]. Finally, tap water with pH of 7.43 was used as mixing water. The detailed chemical composition of the tap water can be found in [29].

2.2. Sample preparation

To study the thixotropic properties of SCPB, a series of SCPB mixtures with fixed solid content (62 %) and binder dosage (7 %) were produced. The mixing efficiency, i.e., the dispersion effect, is important to obtain a homogeneous slurry. Qiu et al. [30] developed a mixing method for CPB with high dispersion efficiency based on the wet packing method [31]. However, due to the extremely high ST content, the agglomeration phenomenon in SCPB is more significant compared to conventional CPB. Therefore, the Qiu method [30] was further refined in this study to be suitable for SCPB preparation. The specific process is as follows:

(a) Mix the required dry ingredients (ST and OPC) for about 2 min;
(b) Divide the dry mixture into two equal parts. Add one portion to the pre-weighed water and mix with a double spiral mixer at low speed (280 r/min) for 4 min;
(c) Divide the remaining dry material into two equal parts again, and subsequently add to the slurry obtained in Step (b) in turn. Note that each addition is followed by 3 min of high-speed mixing.

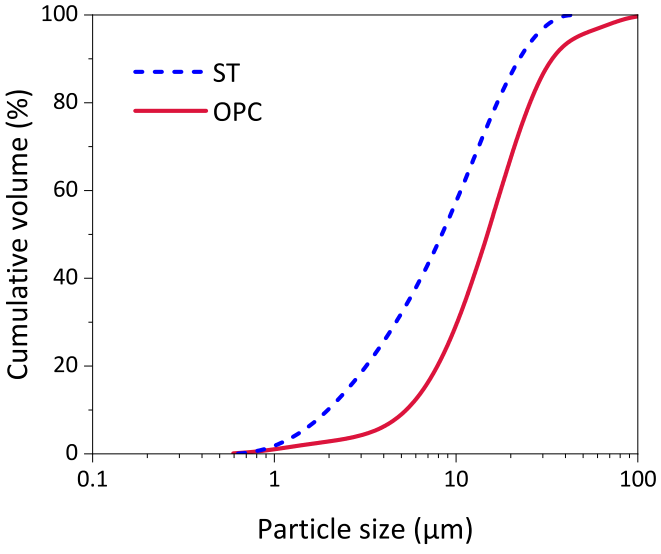

Fig. 1. Particle size distribution curves of ST and OPC.

2.3. Experiments and methods

2.3.1. Rheological tests

In this study, the rotational rheometer (RST-SST, AMETEK Brookfield, U.S.A.) was used for the rheological testing of SCPB. To inhibit the wall-slip effect, a four-blade vane geometry with the height and diameter of 40 and 20 mm, respectively, was chosen. In addition, in order to minimize boundary effects, a cylindrical container of 104 and 140 mm in diameter and height was used.

2.3.1.1. Equilibrium shear test. The prepared fresh SCPB was transferred to the rheometer and then rested for 60 s for the purpose of avoiding residual stress interference caused by this operation [32]. Once the preset resting time was achieved, constant rate shearing was conducted directly until the equilibrium shear stress was obtained. The shear rates selected in this study include 0.1, 1, 10, 40, 70, and 100 s^{-1}. All experiments were performed three times independently to ensure reproducibility of the data.

After obtaining the equilibrium shear stresses corresponding to different shear rates ($\dot{\gamma}$), the dynamic yield stresses were gained using the following conventional non-Newtonian rheological models, respectively.

The Bingham model:

$$\tau = \tau_b + \mu_p \dot{\gamma} \tag{1}$$

where τ and τ_b refer to shear stress and Bingham yield stress, respectively; μ_p is the plastic viscosity,

The Herschel-Bulkley (H-B) model:

$$\tau = \tau_{h-b} + K\dot{\gamma}^n \tag{2}$$

where τ_{h-b} is yield stress obtained from the H-B model; K represents consistency index and n is the H-B index.

The modified Bingham model:

$$\tau = \tau_{m-b} + \mu_p \dot{\gamma} + c\dot{\gamma}^2 \tag{3}$$

where τ_{m-b} is yield stress obtained from the modified Bingham model; c is the coefficient.

2.3.1.2. Shear rate ramp test. To compare with the results of the equilibrium shear test, linear shear rate ramp tests, including short cycle and long cycle tests, were carried out. Similarly, a resting step (60 s) was also conducted prior to the ramp tests. In the short cycle test, the shear rate increases linearly from zero to 100 s^{-1} in 60 s and then decreases to zero over the same time period. As for the long cycle test, the duration of the ramp up or down was 300 s. The detailed measurement process can be seen in Fig. 2.

2.3.1.3. Pre-shear test. Due to the strong thixotropy of SCPB, a pre-shear step is necessary before the start of the formal rheological measurements. After transferring the prepared SCPB into the cylindrical container of the rheometer, the pre-shear step is performed immediately at a constant shear rate of 100 s^{-1} for 10, 200 and 500 s. The corresponding samples are recorded as P10, P200 and P500, respectively.

2.3.1.4. Static yield stress test. The purpose of conducting this test is to obtain the static yield stress of SCPB. The specific procedure is to perform stress growth measurement using a constant shear rate of 0.1 s^{-1}, and the peak stress is defined as the static yield stress. In addition, a shearing duration of 30 s is chosen to ensure that peak stresses can be obtained for all samples during the measurement while minimizing the disturbance of shear on the samples.

2.3.2. Zeta potential test

The zeta potential can provide information about interparticle interactions in suspension and can be used to assess the effect of pore fluid chemistry, which facilitates the analysis of the mechanisms behind rheological behavior of SCPB [24]. The Zetasizer Nano ZS90 (Malvern Panalytical, U.K.) from Malvern Panalytical was used to measure the zeta potential. All samples tested (including SCPB and cement paste, etc.) were diluted to 0.1 g/L. At least three independent tests were performed for each zeta potential measurement to ensure the repeatability of the data.

3. Simple model building

Ferron et al. [33] found that the microstructural response of the fresh cement paste under shear is the combined result of the aggregation and breakage kinetics of the flocs. Flatt and Bowen [34] developed a yield stress model based on the microstructural parameters of the solid percolating network formed by particulate suspensions. Wallevik [35] concluded that the reversible and permanent linkages between cement particles are the dominant reason for the thixotropic behavior of cement paste. Wang et al. [36] observed that the arrangement of particle/agglomerate in CPB is the key to the evolution of rheological properties by the coupled Rheometer-FBRM. This is similar to the phenomenon observed in concrete or cement paste, i.e., the structural state is the result of the coupling of recovery and breakage of particle/agglomerate [37]. These studies suggest that the time- and shear rate-dependent rheological behavior of flocculated suspensions depends on the microstructural evolution [38,39]. Therefore, establishing the relationship between rheological parameters of SCPB and microstructure is the key to modeling.

In view of the above discussion, we first introduced here a dimensionless parameter λ ranging from 0 to 1 to quantify the microstructural level of SCPB. When $\lambda = 1$, it means that all structural components are bonded together, $\lambda = 0$ corresponds to a fully broken structure. The time-dependent λ can be described by the structural kinetics equation as shown in Eq. (4) when the irreversible structural breakage due to shear is reasonably neglected [40]. This equation shows that the break-down rate depends on the shear rate and the degree of structural development,

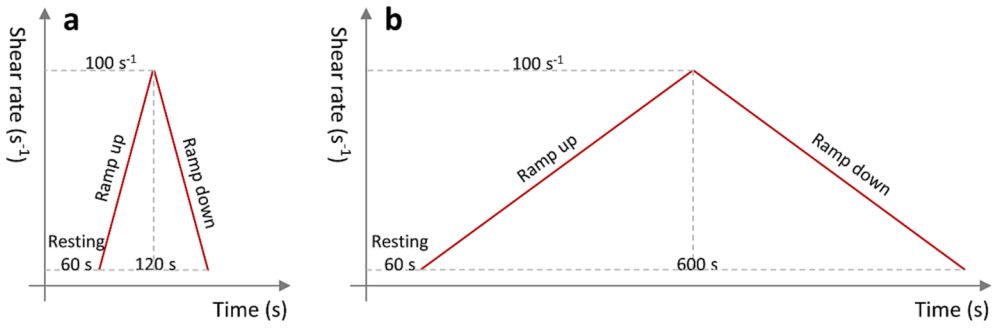

Fig. 2. Flow charts of (a) short cycle test and (b) long cycle test.

while the aggregation or recovery rate is proportional to the distance from the maximum structural parameter (λ_0) [41]. Some models in published literatures such as Roussel model [15,20], Coussot model [42] and Ma model [43] can be considered as a specific form of Eq. (4). Therefore, the evolution equation was also adopted in this study to describe the change rate of the microstructural parameter λ.

$$\frac{d\lambda}{dt} = -k_1\lambda\dot{\gamma} + k_2(\lambda_0 - \lambda) \tag{4}$$

where k_1 and k_2 are the empirical parameters related to break-down and recovery rate, respectively. On this basis, $\frac{1}{k_1\dot{\gamma}}$ and $\frac{1}{k_2}$ represent deflocculation characteristic and flocculation characteristic times, respectively. t is the shearing time, and λ_0 is usually taken as one [41].

When SCPB is in steady state, that is, the rate of break-down equals the recovery rate, the equilibrium structure parameter (λ_e) can be obtained from Eq. (5) as follows:

$$\lambda_e = \frac{k_2}{k_1\dot{\gamma} + k_2} \tag{5}$$

By solving Eq. (5), the general evolution equation of λ for SCPB with time under shear is written as:

$$\lambda = \frac{k_2}{k_1\dot{\gamma} + k_2} + \left(\lambda_{ini} - \frac{k_2}{k_1\dot{\gamma} + k_2}\right)\exp[-(k_1\dot{\gamma} + k_2)t] \tag{6}$$

where λ_{ini} refers to the microstructural level of SCPB before shearing.

After determining the structural kinetic equation, an equation of state is needed to describe the corresponding macroscopic rheological parameters of SCPB at a certain microstructural level [41]. Since SCPB is highly thixotropic, here we divide the shear stress of SCPB into two parts: the steady-state term and the thixotropic term containing the microstructural parameter. The expression is as follows:

$$\tau = \tau_e + \tau_e f(\lambda) \tag{7}$$

where τ_e is the shear stress of SCPB at steady state, its value is only related to the applied strain rate, and the corresponding microstructure level is λ_e; $\tau_e f(\lambda)$ represents the thixotropic term and $f(\lambda)$ is a function of the microstructural parameter associated with thixotropy.

We hypothesize that the ratio of the shear stresses of SCPB in different structural states is equal to that of the corresponding microstructural parameters, from which we can get:

$$\frac{\tau}{\tau_e} = \frac{\lambda}{\lambda_e} = 1 + f(\lambda) \tag{8}$$

Thus Eq. (7) can be further transformed into:

$$\tau = \tau_e + \tau_e\left[\frac{(\lambda - \lambda_e)}{\lambda_e}\right] \tag{9}$$

As for τ_e, it can be expressed using some traditional non-Newtonian rheological models, such as Bingham, H-B and modified Bingham models [15]. Although some studies [25,44] have suggested that the rheological behavior of fresh CPB conforms to the Bingham model, SCPB usually exhibits nonlinear characteristics under shearing [16]. By demonstration (see Section 4.1 for details), the H-B model is more appropriate for characterizing the steady-state rheological behavior of SCPB. Therefore, it is reasonable that the state equation of SCPB can be developed by coupling the H-B model and structural parameter as Eq. (10).

$$\tau = (\tau_{h-b} + K\dot{\gamma}^n) + (\tau_{h-b} + K\dot{\gamma}^n)\left[\frac{(\lambda - \lambda_e)}{\lambda_e}\right] \tag{10}$$

If λ/λ_e is defined as the new structural parameter $\overline{\lambda}$, Eq. (10) can be simplified as

$$\frac{\tau}{\tau_{h-b} + K\dot{\gamma}^n} = \overline{\lambda} \tag{11}$$

It should be noted that Eq. (10) does not apply to conventional CPB, more precisely, the paste whose steady-state rheological behavior does not conform to the H-B model. However, we only need to replace the H-B term in Eq. (10) with the corresponding rheological model (e.g., Bingham model), so the equation of state proposed in this study has strong applicability.

Substituting Eqs. (5) and (6) into Eq. (10), the transient shear stress of thixotropic SCPB can be written as:

$$\tau = (\tau_{h-b} + K\dot{\gamma}^n)\left\{1 + \left(\frac{\lambda_{ini}}{\lambda_e} - 1\right)\exp[-(k_1\dot{\gamma} + k_2)t]\right\} \tag{12}$$

When the SCPB is at rest, the shear rate is zero, and the recovery process is dominant. According to Eq. (12), the static yield stress (τ_{sta}) evolution of SCPB at rest can be further obtained:

$$\tau_{sta} = \tau_{h-b}\left[1 + \left(\frac{\lambda_{ini}}{\lambda_e} - 1\right)\exp(-k_2 t)\right] \tag{13}$$

It is worth noting that Eq. (13) can only describe the initial nonlinear evolution stage of the yield stress of SCPB at rest. Previous studies [23,24] have shown that the static yield stress of CPB increases linearly after the initial evolution stage. Similar results were also observed in cement paste [43] and ultra-high-performance concrete matrix [45]. Therefore, the static yield stress evolution equation of SCPB at rest can finally be written as:

$$\tau_{sta} = \tau_{h-b}\left[1 + \left(\frac{\lambda_{ini}}{\lambda_e} - 1\right)\exp(-k_2 t)\right] + A_{thix}t \tag{14}$$

where A_{thix} refers to the linear evolution rate of static yield stress of SCPB.

4. Determination of model parameters

The parameters to be determined in the equations of state and kinetics include the H-B model rheological parameters (τ_{h-b}, K and n), k_1 and k_2. The rheological parameters of the H-B model can be obtained from the steady state stress response of the SCPB at different constant shear rates, while k_1 and k_2 can be determined from the transient stress response.

4.1. Rheological parameters of H-B model

Looking across the rheological protocols applied in CPB field, previous studies [9,11,21,23,25] mostly used a typical linear shear rate ramp mode. As mentioned before, SCPB is more thixotropic than conventional CPB, which means that the rheological properties of SCPB require a longer shearing time to reach steady flow [35]. Therefore, it is theoretically unreasonable to use the linear shear rate ramp mode for rheological measurements in fresh SCPB. Since the recovery takes significantly more time than breakdown, the rheological measurements in cement-based materials are generally performed by pre-shear to destroy the internal microstructure of the slurry, followed by a stepwise decrease of shear rate, thus reducing the measurement error due to thixotropy [20]. But for SCPB, on the one hand, the microstructural response of SCPB is unclear under different pre-shear conditions, and one of the most direct consequences of this is that the determination of the pre-shear time is arbitrary. The effect of pre-shear is discussed in more detail in Section 5.1. On the other hand, the time for SCPB to reach steady state at the same shear rate is significantly greater than that of cement paste or concrete [19], and the exact duration of each step needed to be further determined. Moreover, the effect of stepwise shear on the steady state of SCPB is also not clear. Therefore, from the perspective of data accuracy, the equilibrium shear test is directly conducted here for obtaining the fitted data of the rheological model, and the linear shear rate ramp test is also conducted for comparison. The results of these two rheological protocols are shown in Fig. 3. For the

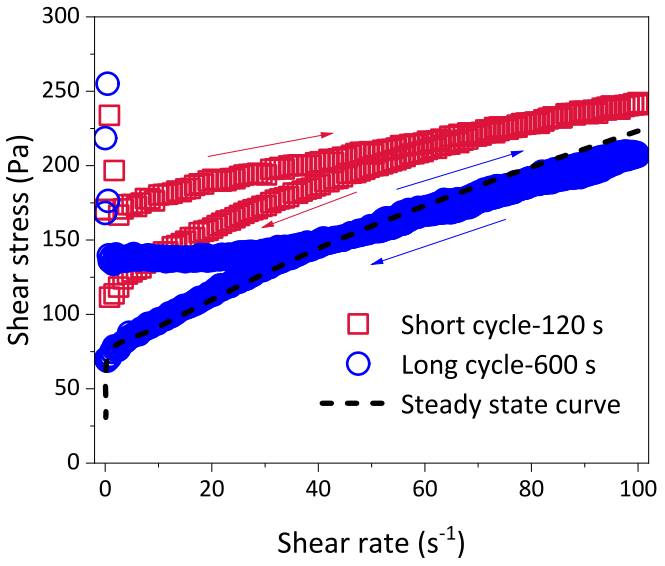

Fig. 3. SCPB flow curves under different rheological protocols.

short cycle test (120 s), all the measured flow curves are above the equilibrium flow curve. This can be attributed to the fact that the shorter shear time fails to bring the sample to a steady state, the flocculation degree in SCPB is higher than that of the equilibrium state at this point [15]. Thus the dynamic yield stress obtained by this protocol is larger than the actual. However, for long measurement cycle (600 s), the ramp down curve shows a rough overlap with the equilibrium flow curve. Although a more realistic dynamic yield stress can be obtained by the equilibrium shear test, this protocol tends to time-, material- and labor-consuming. The above results of linear shear rate ramp tests are interesting, indicating that it is possible to use this rheological protocol to obtain dynamic yield stress in SCPB, and the key lies in the duration of the cycle. However, the specific details need further refinement, for example, in the low shear rate region (less than1 s^{-1}), the long characteristic time for SCPB to reach steady state leads to a significant difference between the corresponding shear stress and the equilibrium stress. Furthermore, as shearing time increases there is a decrease in the hysteresis loop area which corresponds to a decrease in thixotropy degree. This is because the longer the shearing time, the more completely the flocculation structure of the slurry is disrupted. Although Banfill and Saunders [46] suggested that the hydration of the binder may lead to anti-thixotropic behavior in long cycle test. Experimentally, no down-curve was found above the up-curve in SCPB rheological curve. The low binder dosage in SCPB is responsible for this phenomenon.

Fig. 4(a) shows the equilibrium flow curve of SCPB and the fitting results of different rheological models. As can be seen, there exists two parts of the curve. The first one (Region I) shows the SCPB exhibits shear thinning behavior under low shear rate. Beyond the critical shear rate (10 s^{-1}), the shear thinning behavior gradually turns to Bingham behavior, i.e., a constant apparent viscosity with shear rate (Region II). A similar phenomenon was also observed for cement paste [47]. The mechanisms of transition from shear thinning to Bingham behavior can be attributed to the coupling effect of van der Waals attraction and hydrodynamic forces [48]. At the low shear rate range, van der Waals force dominates the hydrodynamic force, a relatively ordered state develops and thus causing a shear thinning macroscopic behavior [49]. It is worth noting that shear thickening, as seen in cementitious paste [50], was not observed in the SCPB within applied shear rate. This may be because the adopted shear rate is not sufficient to reduce the thickness of the diffused layers of the electric double layer on particle surface and thus the structural break-up is still dominant under shearing [51]. This is consistent with the results previously published by Wang et al. [52], they found that the critical shear rate at which CPB begin to exhibit shear thickening is 480 s^{-1}. Some typical non-Newtonian rheological models, including Bingham, H-B and modified Bingham, are used to estimate rheological parameters, and the accuracy of the parameters acquisition depends on the choice of the model [53]. In case of shear-thinning fluids as reported here, the application of the Bingham model leads to the highest yield stress while the lowest yield stress when using the H–B model (Fig. 4(b)). In addition, it is clear that the dynamic yield stresses of SCPB obtained from different rheological models differ significantly, with the largest percentage of difference reaching even 56 %. Therefore, it is necessary to select the rheological model scientifically, so as to ensure the reliability of the obtained rheological parameters of SCPB.

For SCPB, the ideal rheological model can not only fit the shear stress-shear rate data well, but the sensitivity to the nonlinearity of rheological behavior should be as low as possible [54]. The correlation coefficient R^2 was used to evaluate the fitting accuracy of different rheological models. The R^2 obtained from the three different models (Bingham, H-B and modified Bingham models) are 0.9397, 0.9757 and 0.9591 respectively. Hence, from the accuracy of data fitting point of view, the H-B model could provide the most accurate estimation of the rheological parameters of the fresh SCPB. According to the study by Feys et al. [54], the estimated yield stress can be regarded as the most sensitive parameter when various rheological models are considered. Therefore, to estimate the dependence of the rheological models on this

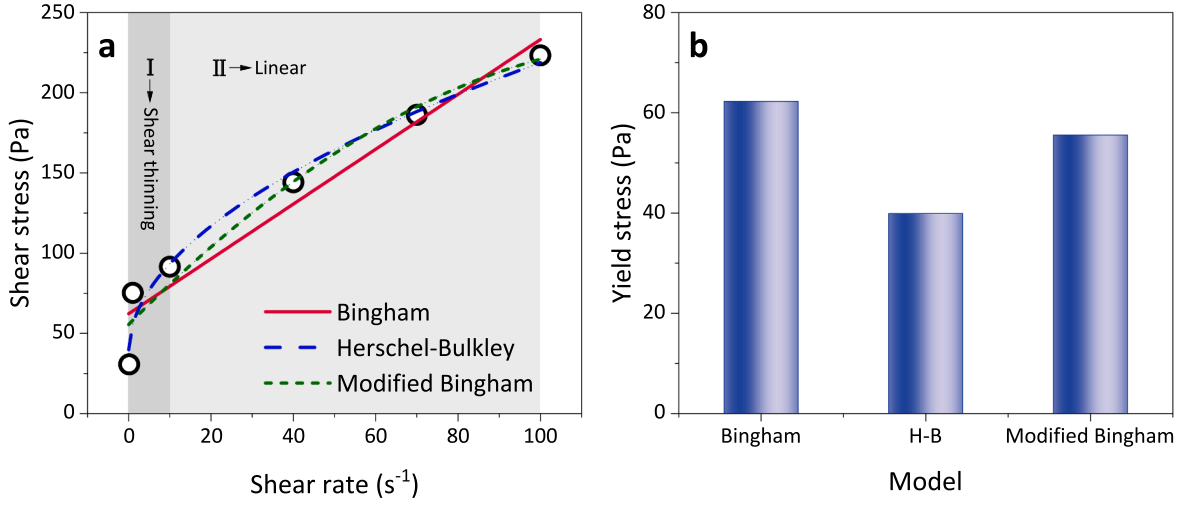

Fig. 4. (a) Steady state flow curve of fresh SCPB. (b) Dynamic yield stresses obtained from different rheological models.

nonlinearity, the ratio of yield stress obtained with different rheological models relative to the calculated yield stress converted by the slump and spread is expressed as a function of the intensity of shear thinning (H-B index, n). In this part, Roussel model [55] and Li model [56] were adopted to obtain the yield stress from the slump and spread flow measurements, respectively. The average of the yield stresses obtained from these two models is taken as the final yield stress to minimize the potential errors associated with the conversion of slump as described in [54]. Fig. 5 displays that only the H-B model shows a constant yield stress ratio (fluctuating slightly around 1) as a function of the n value, indicating that the H-B model appears to be independent of the intensity of shear-thinning. However, it was previously suggested that the modified Bingham model has higher prediction accuracy compared to the H-B model [57]. These differences in results can be attributed to variation in raw materials and mix proportions employed. Collectively, the H-B model is more preferentially recommended to fit rheological data of SCPB considering the accuracy of data fitting and the sensitivity of the intensity of shear thinning. The corresponding dynamic yield stress, consistency index and H-B index are 39.91 Pa, 16.01 and 0.52, respectively. Notably, this conclusion is limited to shear-thinning pastes, and when the paste exhibits shear-thickening as shown in [58], the H-B model may no longer be applicable. The case in [54] provides the classic example. In addition, due to the measurement error of the rheometer and the experimental error of conducting the slump and flow spread tests [54], none of these three models can yield the desired relationship (yield stress ratio = 1).

4.2. k_1 and k_2

The transient shear stress response of the fresh SCPB at constant shear rates of 40 s^{-1} and 70 s^{-1} is depicted in Fig. 6(a). Due to the short shearing duration (100 s), the effect of cement hydration is ignored here. It can be clearly observed that the Eq. (12) fits well with experimental data, which indicates that the proposed model is able to describe the transient flow behavior of SCPB well. Based on the fitting results, k_1 and k_2 can be further obtained by fitting $(k_1\dot{\gamma} + k_2)$ and $\dot{\gamma}$, with results of 10^{-4} and $7.5*10^{-3}$ s^{-1} (Fig. 6(b)), respectively. It is worth noting that Roussel [20] simplified the structural kinetic equations by discarding the build-up term $(k_2(\lambda_0 - \lambda))$ based on the assumption that the characteristic time of de-flocculation is much smaller than the flocculation characteristic time. Obviously, this treatment is not desirable in SCPB. From the experimental results, when the shear rate is 70 s^{-1}, the de-

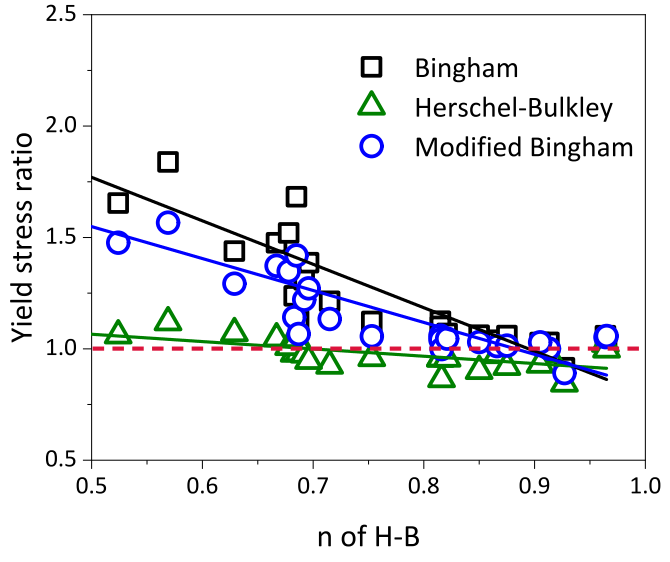

Fig. 5. Evolution of the yield stress ratio as a function of the curvature of the flow curve.

flocculation characteristic time ($\frac{1}{k_1\dot{\gamma}}$) and flocculation characteristic time ($\frac{1}{k_2}$) even reach the same level, which are 142.9 and 133.3 s, respectively.

5. Results and discussion

5.1. Transient flow

According to Eq. (12), in addition to obtaining the rheological parameters of H-B model and kinetic equation coefficients, the key to describing the transient flow of SCPB is the value of the initial structure parameter λ_{ini}, which is usually assumed to be 1 in some literature [43,59]. Based on the results in Section 4, by fitting the shear stress response data of SCPB under pre-shear (100 s^{-1}), λ_{ini} was obtained as 0.926 (Fig. 7(a)), and its fitting accuracy reached 0.923. This shows that the assumption of λ_{ini} as 1 in SCPB is not rigorous. The mixing process during the preparation of SCPB resulted in a more homogeneous slurry, but at the same time caused a certain degree of destruction to the internal structure. Moreover, the process of transferring the sample also caused disturbances to the structure. Ultimately, λ_{ini} is less than 1. Therefore, a pre-shear step is necessary to eliminate the effect of the initial disturbance on the rheological measurements. Under pre-shear, the microstructural parameter of SCPB decreases from λ_{ini} to the equilibrium value (λ_e) following Eq. (6). It should be realized that λ_e is not equal to zero. For example, when the constant shear rate is 100 s^{-1}, the corresponding λ_e at structural equilibrium is 0.429. It is entirely reasonable, when the structure is in equilibrium, it only means flocculation and deflocculation balance, and does not mean that the slurry is in a fully dispersed state. The fact that the slurry can still able to support a high shear stress at equilibrium is a good proof of the above point. For ease of comparison, λ is normalized ($\lambda' = (\lambda - \lambda_e)/(\lambda_{ini} - \lambda_e)$), and its value is in the range from 0 to 1. Similarly, the higher the value, the more fully developed the structure is. Residual structural parameter (λ') at the end of different pre-shear times (P10, P200 and P500) are shown in Fig. 7(b). Obviously, smaller pre-shear duration leaves a more intact structure. When the pre-shear time is 500 s, the microstructure of SCPB is basically destroyed at this time, i.e., the slurry reached the so-called the same reproducible reference state. This provides a reference for the selection of pre-shear parameters for rheological measurements of SCPB. But at the same time, there is no doubt that 500 s pre-shear time is a surprisingly high value for the rheological measurement of conventional CPB. For example, Jiang et al. [44] used a pre-shear time of only 120 s when studying the effect of mineral admixtures on the rheological properties of CPB. This again demonstrates the difference in thixotropy between SCPB and traditional CPB. After reaching the preset pre-shear time, a strain rate equal to 0.1 s^{-1} was then applied to the SCPB, and the results are shown in Fig. 7(a). The shear stress instantaneously drops to a lower value (static initial stress) due to the inelastic thixotropy [40]. Furthermore, as expected, higher λ' leads to higher static initial stress, which is consistent with the microstructural level of SCPB.

The transient flow response of SCPB under 0.1 s^{-1} shear is presented in Fig. 8(a). The obtained curve can be divided into two phases. The first phase is a decrease in stress from a peak. It is followed by an equilibrium stress which corresponds to a steady state regime. Since the relatively high pre-shear rate, those early hydrates bridges (at pseudo-contact points) as well as the colloidal network formed by the non-contact colloidal interaction are broken down [60], and more specifically, the static yield stress of SCPB has been overcome in the pre-shear stage. Therefore, at the beginning of the static yield stress test, the shear stress of SCPB does not show a linear growth phase, but directly decreases to its new steady state. The proposed model is able to predict this phenomenon. All the samples tend towards the same steady state no matter what the pre-shear duration is. The shear stress corresponding to this stable state is about 44.7 Pa, which indicates that pre-shear time does not affect the stable state of SCPB under the specific shear rate. This is in

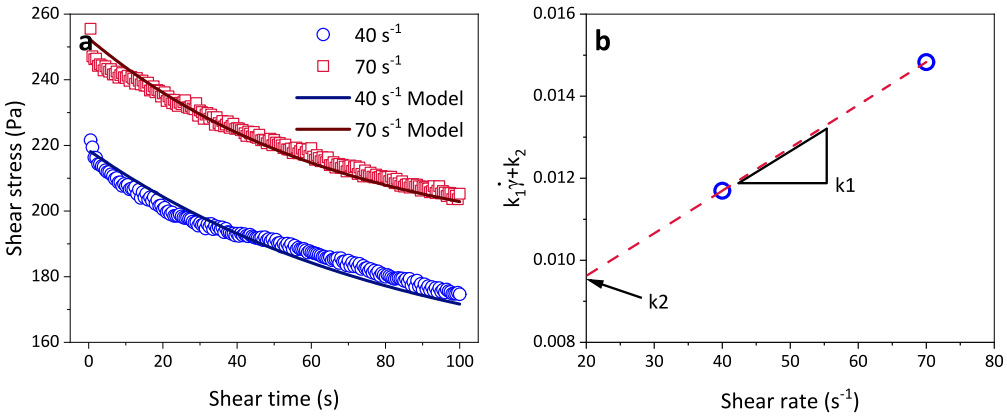

Fig. 6. (a) Shear stress-time transient behavior for SCPB and the fitting result by Eq. (12). (b) Determination of k_1 and k_2.

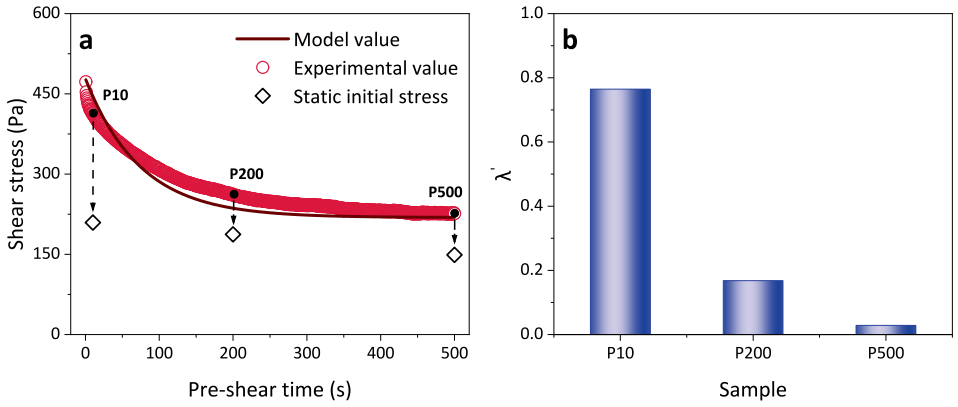

Fig. 7. (a) Shear stress evolution in SCPB under pre-shear. (b) Residual structural parameters of SCPB after different pre-shear durations.

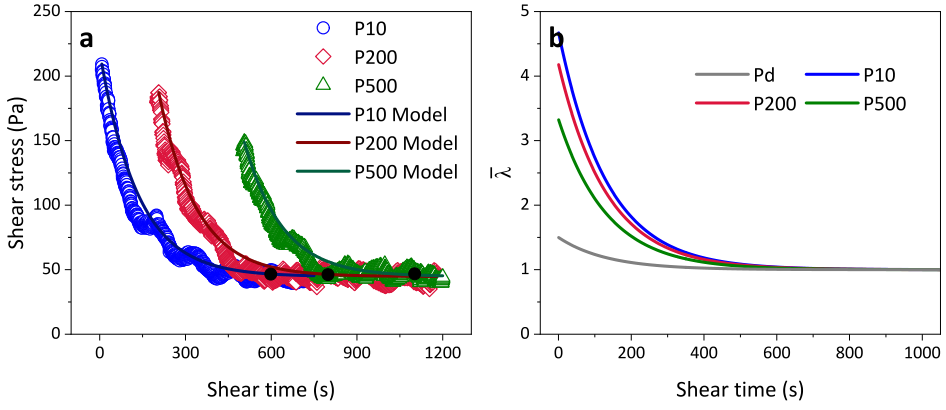

Fig. 8. (a) Shear stress and (b) $\bar{\lambda}$ evolution of SCPB for different pre-shear durations under 0.1 s^{-1}.

accordance with the model as the structure parameter $\bar{\lambda}$ eventually reaches a value of 1 under constant shear rates. In addition, the aging effect caused by cement hydration was negligible for at least 1200 s. This is in sharp contrast to what was observed in fresh cement paste, where cement hydration has an irreversible effect on the rheological properties of the slurry within a few tens of minutes [15]. The low percentage of cement in SCPB is the main reason for this phenomenon. Fig. 8(b) shows the evolution of $\bar{\lambda}$ obtained using the model of this study (Eq. (12)). As expected, $\bar{\lambda}$ decreases with shear time. However, from the figure, the pre-shear time does not seem to affect the time required for the SCPB to reach the equilibrium state, with all samples reaching steady state at around 600 s. The model results are also consistent with the experimental data, with P10, P200 and P500 reaching equilibrium at approximately 600 s, 800 s and 1100 s as shown in Fig. 8(a), respectively. Roussel [15] suggested that for samples with the same steady state structural parameters, a larger initial structural parameter leads to an increase in the time required for the cement paste to reach the steady state. This is another difference between SCPB and cement paste. According to Eq. (6), although larger initial structural parameter will increase the decay rate of $\bar{\lambda}$, the effect is limited, so there is little difference in the time required for each sample to reach equilibrium. However, after careful comparison, it can be seen from Fig. 8(b) that P500 reaches equilibrium slightly earlier than P10 and P200. If the initial $\bar{\lambda}$ is chosen to be 1.5, it can be seen that the time for the SCPB (Pd) to reach

equilibrium is obviously shortened to 400 s. It can therefore be inferred that the time to equilibrium of SCPB can be significantly shortened if the initial $\bar{\lambda}$ is significantly reduced by the pre-shear process. Regrettably, however, this method has limited effectiveness, as seen in the experimental results. For example, for P10 and P500, there was no significant difference in the time for the samples to reach equilibrium, despite the 4900 % increase in shear time. This is primarily because the low dispersion efficiency of shearing on the structure in the later stage, which is also illustrated by the residual structural parameter of samples after different pre-shear times. The stepwise shear mode may be a more efficient approach because the high dispersion effects of different constant shear effects can be continuously superimposed. This is also the reason why the long cycle test can yield similar results to the equilibrium shear test in Section 4.1.

5.2. Time-dependent static yield stress

The measured and predicted static yield stress are plotted in Fig. 9(a) as a function of the resting time. Good fitting with the proposed nonlinear model (Eq. (14)) supports that there are two kinetics of structural build-up for SCPB at rest: structure evolves slowly at first and then increases linearly. This is consistent with the result reported by Xu et al. [61]. However, the initial evolution stage of static yield stress is in disagreement with studies by Rousse [15] and Ma et al. [43]. They observed the structure evolves rapidly at first. The static yield stress evolution of cement-based materials at early age (1800 s in this study) is related to the degree of flocculation [45]. Although the fine particles in SCPB will flocculate immediately after the shear step due to the particle–particle interactions, thus increasing the yield stress macroscopically. It is worth noting that the surface activity of the tailings is mainly derived from two sources: a) residual mineral processing agents such as flocculants on the particle surface, and b) the adhesion of cement hydration products such as CSH and ettringite. However, tailings can still be regarded as inert particles compared with cement, and the flocculation characteristic time of tailings is much longer than that of cement [16], and its flocculation strength is also far weaker than that of cement flocculation. These differences can be mainly attributed to the difference in the particle surface charges. This is supported by the in-situ zeta potential measurements evidences carried out on OPC, iron tailings and SCPB with results of − 6.6, −26.5 and − 20.8 mV, respectively. The SCPB samples exhibit a higher negative zeta potential than OPC, thus resulting in weaker flocculation compared to cement paste [28]. Similar observation was also observed by Xue et al. [13]. Another point which should be noted is that the SCPB with a longer shearing time has a lower static yield stress within the resting time studied. This seems to contradict the conclusion reached by Liu and Fall [27], who found that longer mixing time led to higher yield stress of CPB. The reason for this phenomenon is mainly the initial static yield stress ($\tau_{sta,0}$) jump and A_{thix} decrease. Fig. 9(b) shows $\tau_{sta,0}$ and A_{thix} as a function of λ'. Apparently, lower λ', corresponding to longer shearing duration, leads to lower $\tau_{sta,0}$ and A_{thix}. On the one hand, the longer the shearing duration, the more incomplete the slurry structure is. Roussel et al. [18] believed that the early static yield stress of cement paste is the shear stress corresponding to the maximum critical strain related to colloid interaction. Although, as described in some studies [27,62], longer shear time means higher hydration product volume, flocculation formed by colloidal interaction at this time is still the dominant factor of SCPB static yield stress. Thus $\tau_{sta,0}$ decreases with the shearing duration. On the other hand, longer shear time may increase the particle separation and thus slow down the hydration nucleation rate [43], i.e., the reduction of A_{thix}. All combined, this eventually leads to a decrease in the static yield stress of SCPB with shear time.

To further understand the effect of shear time on the particle surface charges, the zeta potential of the samples (P10, P200 and P500) are presented in Fig. 9(c). It can be clearly seen that the absolute value of the zeta potential increases with shear time. The higher the surface charge means a stronger interparticle repulsion and therefore a weaker flocculation [63]. This agrees with the $\tau_{sta,0}$ results, indicating a weaker slurry structure with shear time. The larger interparticle repulsion also indicates a larger bridging distance, which reduces the number of pseudo-contact points, and thus leads to a decrease in the hydration nucleation rate [17]. This further validates the above speculation about the reason for the decrease of A_{thix}.

6. Conclusions

In this study, a simple thixotropy model was proposed to describe the transient flow and time-dependent yield stress of SCPB. In addition, the effect of pre-shear time on the rheological behavior of SCPB was also evaluated. The following are the main conclusions obtained:

1. The dynamic yield stresses of SCPB obtained from different rheological models vary widely and the H-B model can provide the most stable dynamic yield stress estimation. In addition, there is potential to use the linear shear rate ramp protocol to obtain dynamic yield stress of SCPB, where the key lies in the duration of the cycle.
2. The pre-shear time did not affect the steady state of SCPB at a specific shear rate. A longer pre-shear duration (within 500 s), associated with a more incomplete microstructure, resulted in a smaller initial static yield stress ($\tau_{sta,0}$) and delayed static yield stress recovery kinetics (A_{thix}). But at the same time there is little difference in the time required for SCPB samples to reach steady state due to the influence of later dispersion efficiency.
3. The proposed model exhibited good fitting with the transient behavior and static yield stress evolution of SCPB. The static yield stress of SCPB presented a slow growth followed by a rapid linear increase with resting time under the combined effect of colloidal interaction and hydration nucleation rate.

It should be noted that we related the microstructure of SCPB by introducing the dimensionless parameter λ, but it is undeniable that λ is

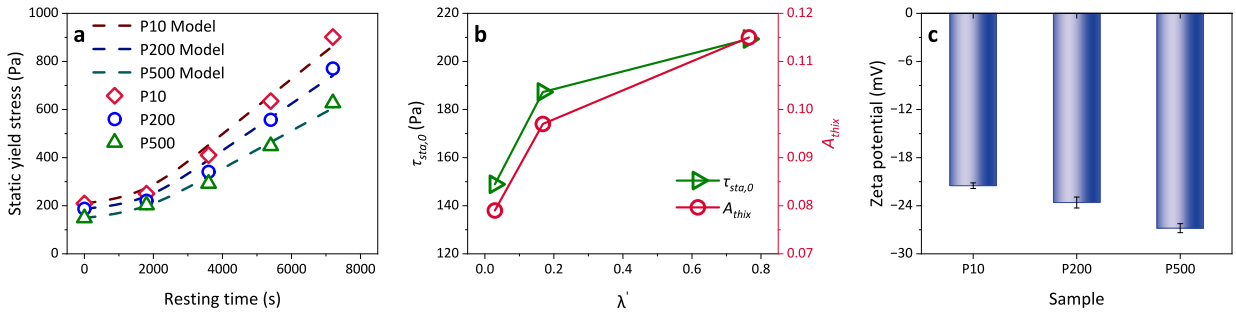

Fig. 9. (a) Measured and predicted static yield stress as function of the resting time. (b) $\tau_{sta,0}$ and A_{thix} as a function of λ'. (c) Zeta potential of samples after different pre-shear times.

abstract. Furthermore, there are some assumptions based on experimental results in the derivation of the model. Therefore, in future work, it is necessary to relate quantitative indicators with practical physical meaningful to the model parameters and to carry out more mathematical derivations to make the model more scientifically rigorous.

CRediT authorship contribution statement

Zhenbang Guo: Methodology, Validation, Formal analysis, Investigation, Writing – original draft. **Jingping Qiu:** Resources, Validation. **Haiqiang Jiang:** Validation, Investigation, Writing – review & editing. **Qiang Zhu:** Validation, Investigation, Writing – review & editing. **Jin Wang Kwek:** Validation, Investigation, Writing – review & editing. **Lin Ke:** Validation, Investigation, Writing – review & editing. **Zhengyao Qu:** Conceptualization, Resources, Supervision, Writing – review & editing.

Declaration of Competing Interest

The authors declare that they have no known competing financial interests or personal relationships that could have appeared to influence the work reported in this paper.

Data availability

Data will be made available on request.

Acknowledgments

Financial supports by Key Research and Development Project of Liaoning (2020JH1/10300005), National Key Research and Development Program (2019YFC1907202), and China Scholarship Council (No. 202206080032) are greatly appreciated. The authors also would like to thank Fan Yao from Shiyanjia Lab (www.shiyanjia.com) for technical support of rheological tests.

References

[1] M. Fall, M. Benzaazoua, S. Ouellet, Experimental characterization of the influence of tailings fineness and density on the quality of cemented paste backfill, Miner. Eng. 18 (1) (2005) 41–44.
[2] L. Liu, Z. Fang, C. Qi, B. Zhang, L. Guo, K.-I.-I.-L. Song, Numerical study on the pipe flow characteristics of the cemented paste backfill slurry considering hydration effects, Powder Technol. 343 (2019) 454–464.
[3] L. Yang, E. Yilmaz, J. Li, H. Liu, H. Jiang, Effect of superplasticizer type and dosage on fluidity and strength behavior of cemented tailings backfill with different solid contents, Constr Build Mater. 187 (2018) 290–298.
[4] C. Qi, A. Fourie, Q. Chen, Q. Zhang, A strength prediction model using artificial intelligence for recycling waste tailings as cemented paste backfill, J Clean Prod. 183 (2018) 566–578.
[5] Q. Chen, Y. Tao, Q. Zhang, C. Qi, The rheological, mechanical and heavy metal leaching properties of cemented paste backfill under the influence of anionic polyacrylamide, Chemosphere. 286 (2022), 131630.
[6] S. Chakilam, L. Cui, Effect of polypropylene fiber content and fiber length on the saturated hydraulic conductivity of hydrating cemented paste backfill, Constr Build Mater. 262 (2020), 120854.
[7] W. Xu, Q. Li, B. Liu, Coupled effect of curing temperature and age on compressive behavior, microstructure and ultrasonic properties of cemented tailings backfill, Constr Build Mater. 237 (2020), 117738.
[8] Q. Chen, L. Zhu, Y. Wang, J. Chen, C. Qi, The carbon uptake and mechanical property of cemented paste backfill carbonation curing for low concentration of CO2, Sci. Total Environ. 852 (2022) 158516.
[9] X. Deng, B. Klein, L. Tong, B. de Wit, Experimental study on the rheological behavior of ultra-fine cemented backfill, Constr Build Mater. 158 (2018) 985–994.
[10] X. Chen, X. Shi, J. Zhou, X. Du, Q. Chen, X. Qiu, Effect of overflow tailings properties on cemented paste backfill, J. Environ. Manage. 235 (2019) 133–144.
[11] Z. Guo, J. Qiu, H. Jiang, J. Xing, X. Sun, Z. Ma, Flowability of ultrafine-tailings cemented paste backfill incorporating superplasticizer: Insight from water film thickness theory, Powder Technol. 381 (2021) 509–517.
[12] B. Liu, Y.-T. Gao, A.-B. Jin, X. Wang, Influence of water loss on mechanical properties of superfine tailing–blast-furnace slag backfill, Constr. Build. Mater. 246 (2020), 118482.
[13] Z. Xue, D. Gan, Y. Zhang, Z. Liu, Rheological behavior of ultrafine-tailings cemented paste backfill in high-temperature mining conditions, Constr. Build. Mater. 253 (2020), 119212.
[14] Y. Zhang, D. Gan, Z. Xue, H. Lu, Novel testing method for thixotropy of paste slurry with respect to influencing factors and rheological parameters, Adv. Powder Technol. 32 (12) (2021) 4744–4753.
[15] N. Roussel, Steady and transient flow behaviour of fresh cement pastes, Cem Concr Res. 35 (9) (2005) 1656–1664.
[16] Z. Guo, X. Sun, X. Zhang, J. Qiu, H. Jiang, Y. Zhao, P. Wu, Q.i. Zhang, Effect of superplasticizer on rheology and thixotropy of superfine-tailings cemented paste backfill: experiment and modelling, Constr. Build. Mater. 316 (2022) 125693.
[17] D. Lowke, Thixotropy of SCC—A model describing the effect of particle packing and superplasticizer adsorption on thixotropic structural build-up of the mortar phase based on interparticle interactions, Cem. Concr. Res. 104 (2018) 94–104.
[18] N. Roussel, G. Ovarlez, S. Garrault, C. Brumaud, The origins of thixotropy of fresh cement pastes, Cem. Concr. Res. 42 (1) (2012) 148–157.
[19] H. Cheng, S. Wu, H. Li, X. Zhang, Influence of time and temperature on rheology and flow performance of cemented paste backfill, Constr. Build. Mater. 231 (2020), 117117.
[20] N. Roussel, A thixotropy model for fresh fluid concretes: theory, validation and applications, Cem. Concr. Res. 36 (10) (2006) 1797–1806.
[21] X.J. Deng, B. Klein, D.J. Hallbom, B. de Wit, J.X. Zhang, Influence of particle size on the basic and time-dependent rheological behaviors of cemented paste backfill, J. Mater. Eng. Perform. 27 (7) (2018) 3478–3487.
[22] X.J. Deng, B. Klein, J.X. Zhang, D. Hallbom, B. de Wit, Time-dependent rheological behaviour of cemented backfill mixture, Int. J. Min. Reclam Environ. 32 (3) (2018) 145–162.
[23] W. Xu, M. Tian, Q. Li, Time-dependent rheological properties and mechanical performance of fresh cemented tailings backfill containing flocculants, Miner. Eng. 145 (2020), 106064.
[24] S. Haruna, M. Fall, Time- and temperature-dependent rheological properties of cemented paste backfill that contains superplasticizer, Powder Technol. 360 (2020) 731–740.
[25] Y. Kou, H. Jiang, L. Ren, E. Yilmaz, Y. Li, Rheological properties of cemented paste backfill with alkali-activated slag, Minerals 10 (2020) 1–14.
[26] L. Yang, H. Wang, A. Wu, H. Li, T.A. Bruno, X. Zhou, X. Wang, Effect of mixing time on hydration kinetics and mechanical property of cemented paste backfill, Constr. Build. Mater. 247 (2020), 118516.
[27] S.-G. Liu, M. Fall, Fresh and hardened properties of cemented paste backfill: Links to mixing time, Constr. Build. Mater. 324 (2022) 126688.
[28] H. Jiang, Z. Qi, E. Yilmaz, J. Han, J. Qiu, C. Dong, Effectiveness of alkali-activated slag as alternative binder on workability and early age compressive strength of cemented paste backfills, Constr. Build. Mater. 218 (2019) 689–700.
[29] J. Qiu, Z. Guo, L. Yang, H. Jiang, Y. Zhao, Effect of tailings fineness on flow, strength, ultrasonic and microstructure characteristics of cemented paste backfill, Constr. Build. Mater. 263 (2020), 120645.
[30] J. Qiu, Z. Guo, L. Yang, H. Jiang, Y. Zhao, Effects of packing density and water film thickness on the fluidity behaviour of cemented paste backfill, Powder Technol. 359 (2020) 27–35.
[31] H.H.C. Wong, A.K.H. Kwan, Packing density of cementitious materials: Part 1-measurement using a wet packing method, Materials and Structures/Materiaux et, Constructions 41 (2008) 689–701.
[32] M.F. Alnahhal, T. Kim, A. Hajimohammadi, Distinctive rheological and temporal viscoelastic behaviour of alkali-activated fly ash/slag pastes: a comparative study with cement paste, Cem. Concr. Res. 144 (2021), 106441.
[33] R.D. Ferron, S. Shah, E. Fuente, C. Negro, Aggregation and breakage kinetics of fresh cement paste, Cem. Concr. Res. 50 (2013) 1–10.
[34] R.J. Flatt, P. Bowen, Yodel: a yield stress model for suspensions, J. Am. Ceram. Soc. 89 (4) (2006) 1244–1256.
[35] J.E. Wallevik, Rheological properties of cement paste: thixotropic behavior and structural breakdown, Cem. Concr. Res. 39 (1) (2009) 14–29.
[36] H. Wang, L. Yang, H. Li, X.u. Zhou, X. Wang, Using coupled rheometer-FBRM to study rheological properties and microstructure of cemented paste backfill, Adv. Mater. Sci. Eng. 2019 (2019) 1–10.
[37] F. Moore, The rheology of ceramic slip and bodies, Trans. Brit. Ceram. Soc. 58 (1959) 470–492.
[38] Z.M. Png, X.Y.D. Soo, M.H. Chua, P.J. Ong, A. Suwardi, C.K.I. Tan, J. Xu, Q. Zhu, Strategies to reduce the flammability of organic phase change materials: a review, Solar Energy. 231 (2022) 115–128.
[39] V.P. Bui, H.Z. Liu, Y.Y. Low, T. Tang, Q. Zhu, K.W. Shah, E. Shidoji, Y.M. Lim, W. S. Koh, Evaluation of building glass performance metrics for the tropical climate, Energy Build. 157 (2017) 195–203.
[40] J. Mewis, N.J. Wagner, Thixotropy, Adv. Colloid Interface Sci. 147 (2009) 214–227.
[41] E.A. Toorman, Modelling the thixotropic behaviour of dense cohesive sediment suspensions, Rheol Acta. 36 (1) (1997) 56–65.
[42] P. Coussot, Q.D. Nguyen, H.T. Huynh, D. Bonn, Avalanche behavior in yield stress fluids, Phys. Rev. Lett. 88 (2002), 175501.
[43] S. Ma, Y. Qian, S. Kawashima, Experimental and modeling study on the non-linear structural build-up of fresh cement pastes incorporating viscosity modifying admixtures, Cem. Concr. Res. 108 (2018) 1–9.
[44] H. Jiang, M. Fall, E. Yilmaz, Y. Li, L. Yang, Effect of mineral admixtures on flow properties of fresh cemented paste backfill: assessment of time dependency and thixotropy, Powder Technol. 372 (2020) 258–266.
[45] L.e. Teng, J. Zhu, K.H. Khayat, J. Liu, Effect of welan gum and nanoclay on thixotropy of UHPC, Cem. Concr. Res. 138 (2020) 106238.

[46] P.F.G. Banfill, D.C. Saunders, On the viscometric examination of cement pastes, Cem. Concr. Res. 11 (3) (1981) 363–370.
[47] D. Jiao, K. Lesage, M.Y. Yardimci, K. El Cheikh, C. Shi, G. De Schutter, Rheological behavior of cement paste with nano-Fe3O4 under magnetic field: magneto-rheological responses and conceptual calculations, Cem. Concr. Compos. 120 (2021) 104035.
[48] A.M. Mostafa, P. Diederich, A. Yahia, Effectiveness of rotational shear in dispersing concentrated cement suspensions, J. Sustain Cem. Based Mater. 4 (3-4) (2015) 205–214.
[49] N. Roussel, A. Lemaître, R.J. Flatt, P. Coussot, Steady state flow of cement suspensions: a micromechanical state of the art, Cem. Concr. Res. 40 (1) (2010) 77–84.
[50] D. Jiao, C. Shi, Q. Yuan, Time-dependent rheological behavior of cementitious paste under continuous shear mixing, Constr. Build. Mater. 226 (2019) 591–600.
[51] D. Han, R.D. Ferron, Influence of high mixing intensity on rheology, hydration, and microstructure of fresh state cement paste, Cem. Concr. Res. 84 (2016) 95–106.
[52] L. Yang, H. Wang, A. Wu, H. Li, A.B. Tchamba, T.A. Bier, Shear thinning and thickening of cemented paste backfill, Appl. Rheol. 29 (2019) 80–93.
[53] O.H. Wallevik, D. Feys, J.E. Wallevik, K.H. Khayat, Avoiding inaccurate interpretations of rheological measurements for cement-based materials, Cem Concr Res. 78 (2015) 100–109.
[54] D. Feys, J.E. Wallevik, A. Yahia, K.H. Khayat, O.H. Wallevik, Extension of the Reiner-Riwlin equation to determine modified Bingham parameters measured in coaxial cylinders rheometers, Mater Struct. 46 (1-2) (2013) 289–311.
[55] N. Roussel, P. Coussot, "Fifty-cent rheometer" for yield stress measurements: from slump to spreading flow, J. Rheol. (N Y N Y). 49 (3) (2005) 705–718.
[56] W. Li, L. Guo, G. Liu, A. Pan, T. Zhang, Analytical and experimental investigation of the relationship between spread and yield stress in the mini-cone test for cemented tailings backfill, Constr. Build. Mater. 260 (2020), 119770.
[57] A. Yahia, K.H. Khayat, Applicability of rheological models to high-performance grouts containing supplementary cementitious materials and viscosity enhancing admixture, Mater. Struct. 36 (6) (2003) 402–412.
[58] D. Ouattara, M. Mbonimpa, A. Yahia, T. Belem, Assessment of rheological parameters of high density cemented paste backfill mixtures incorporating superplasticizers, Constr. Build. Mater. 190 (2018) 294–307.
[59] D. Wang, Y. Zhang, J. Xiao, T. Huang, M. Wu, S. Zuo, Y. Yang, Structural kinetics constitutive models for characterizing the time-dependent rheologic behaviors of fresh cement paste, Constr. Build. Mater. 276 (2021), 122175.
[60] Y. Qian, S. Kawashima, Use of creep recovery protocol to measure static yield stress and structural rebuilding of fresh cement pastes, Cem. Concr. Res. 90 (2016) 73–79.
[61] W. Xu, Y. Zhang, X. Zuo, M. Hong, Time-dependent rheological and mechanical properties of silica fume modified cemented tailings backfill in low temperature environment, Cem. Concr. Compos. 114 (2020), 103804.
[62] L. Yang, H. Wang, H. Li, X. Zhou, Effect of high mixing intensity on rheological properties of cemented paste backfill, Minerals 9 (2019) 240.
[63] Y. Elakneswaran, T. Nawa, K. Kurumisawa, Zeta potential study of paste blends with slag, Cem. Concr. Compos. 31 (1) (2009) 72–76.